

2022-09-14

A novel tool for quantitative measurement of distortion in keratoconus

Joshi, Mahesh Raj

<http://hdl.handle.net/10026.1/19897>

10.1038/s41433-022-02240-x

Eye

Springer Science and Business Media LLC

All content in PEARL is protected by copyright law. Author manuscripts are made available in accordance with publisher policies. Please cite only the published version using the details provided on the item record or document. In the absence of an open licence (e.g. Creative Commons), permissions for further reuse of content should be sought from the publisher or author.

1 **A novel tool for quantitative measurement of distortion in keratoconus**

2 **Mahesh R Joshi¹, Kenrick J Voison², Marianne Coleman³, Niall Farnon², Peter Bex⁴**

3 **Affiliations:** ¹ Eye and Vision Research Group, School of Health Professions, University of Plymouth,
4 Plymouth, United Kingdom

5 ² Optometry Unit, Faculty of Health, St. Augustine Campus, The University of the West Indies, St. Augustine,
6 Trinidad & Tobago

7 ³ Department of Optometry and Vision Sciences, University of Melbourne, Victoria, Australia

8 ⁴ Psychology Department, Northeastern University, Boston, USA

9
10 **Corresponding author:** Mahesh R Joshi; Mahesh.Joshi@plymouth.ac.uk

11
12 **Abstract**

13 **Background:** Keratoconus is associated with thinning and anterior protrusion of the cornea resulting
14 in the symptoms of blurry and distorted vision. The commonly used clinical vision tests such as visual
15 acuity and contrast sensitivity may not reflect the symptoms experienced in keratoconus and there are
16 no quantitative tools to measure visual distortion. In this study, we used a quantitative test based on
17 vernier alignment and field matching techniques to quantify visual distortion in keratoconus and
18 assess its relation to corneal structural changes.

19 **Methods:** A total of 50 participants (25 keratoconus and 25 visually normal) completed the
20 experiment where they aligned supra-threshold white target circles in opposite field in reference to
21 guide lines and circles to complete a square structure. The task was repeated five times and the global
22 distortion index (GDI) and global uncertainty index (GUI) were calculated as the mean and standard
23 deviation respectively of local perceived misalignment of target circles over five trials.

24 **Results:** Both GDI and GUI were higher in participants with keratoconus compared to controls ($p <$
25 0.01). Both parameters correlated with the best corrected visual acuity, maximum corneal curvature
26 (K_{max}), topographical keratoconus classification (TKC) and central corneal thickness (CCT).

27 **Conclusion:** Our findings show that the quantitative measure of distortion could be a useful tool for
28 behavioural assessment of progressive keratoconus.

29 **Introduction**

30 Keratoconus is a progressive corneal condition characterised by anterior protrusion and thinning of
31 the cornea. The aetiology of the condition is multifactorial with recent studies suggesting a role of
32 inflammatory mechanisms.(1, 2) The estimated prevalence of keratoconus is reported to be 1 in 84
33 (3) to 1 in 375 (4) in young adults. The condition has a genetic heterogeneity and involves both
34 autosomal dominant and autosomal recessive patterns.(5) The corneal structural changes lead to
35 irregular astigmatism and myopia with the symptoms of blurry vision, increased sensitivity to glare,
36 and distorted vision due to higher order aberrations.(6-8) The symptoms begin in adolescence or early
37 adulthood and usually slowly progresses until mid-adulthood.(8)

38

39 The commonly assessed structural measurements in keratoconus include corneal curvature, corneal
40 topography, and corneal thickness using keratometer, corneal topographer, and ocular coherence
41 tomogram (OCT) respectively. Visual acuity is the most commonly measured visual function
42 outcome in the clinical setup. However, visual acuity is not a good predictor of symptoms experienced
43 in keratoconus and vision related quality of life is reduced even in early stages of the disorder while
44 good visual acuity may be maintained. (9-12) Contrast sensitivity meanwhile correlates both with
45 higher order aberration (7, 13) and topographic indices (14). However, clinically available contrast
46 sensitivity charts may not be appropriate for the evaluation of moderate to advanced keratoconus. (15)
47 Hence there is a lack of a perceptual visual measure that reflects symptoms experienced in
48 keratoconus. Different parameters indicate keratoconus progression, and therefore need for
49 intervention with methods such as collagen cross-linking. These include an increase in maximum
50 corneal curvature by 1 D over a year (16), increase in astigmatism by 1 - 3 DC over 6 months, and
51 reduction in central corneal thickness by 5% over 6 months (17). Previous studies have demonstrated
52 variable correlation of best-corrected visual acuity with these parameters, with contrast sensitivity
53 again showing a better correlation.(18, 19) However, monitoring clinical progression requires
54 specialist imaging equipment, and therefore regular visits to an eye care professional are required.
55 Recently a new scoring system that includes clinical measures and the patient characteristics such as
56 patient reported quality of vision, the Dutch Crosslinking for Keratoconus Score, is reported to be

57 better at predicting when medical intervention may be needed.(20) A reliable perceptual
58 measurement that better reflects patient's visual status may further aid development of such scoring
59 system. Such a measure could also potentially be used as a home-based test.

60

61 While visual distortion is one of the most common symptoms in keratoconus, there are currently
62 limited methods to quantify such distortion and none as far as we are aware specifically designed for
63 keratoconus. There have been approaches to quantify distortion using hyperacuity tasks in different
64 ocular conditions. (21-24) Hyperacuity refers to the visual system's ability to perform spatial tasks
65 beyond the eye's classical resolution limit with thresholds as low as 3 to 6 secs of arc. (25, 26) Vernier
66 alignment (vernier acuity), a classic hyperacuity task where participants discriminate difference in the
67 relative spatial localisation of two or more visual stimuli such as lines or dots has been used in
68 previous studies (27-29). The use of such methods for conditions such as amblyopia (30) and age-
69 related macular degeneration (AMD) (31) have demonstrated perceptual distortions exhibit a similar
70 dissociation from visual acuity as clinical keratoconus indices. Thus, evaluating perceptual distortions
71 may provide a more nuanced characterisation of visual function for ocular diseases.

72

73 In this study, we used a quantitative paradigm based on both vernier alignment and field matching
74 techniques to quantify visual distortion experienced in keratoconus and assess its relation to corneal
75 structural changes. Providing a means to reliably and systematically characterise the visual deficit in
76 keratoconus enables future studies exploring the impact of established treatments upon these deficits.

77

78 **Methods**

79 **Participants:**

80 A total of 25 participants (mean age = 29.84 ± 7.46 years, 15 females) with keratoconus at different
81 disease stages and 25 normal controls (mean age = 22.12 ± 2.62 years, 17 females) were recruited for
82 the study. All participants underwent measurements of the best-corrected monocular visual acuity
83 (BCVA) with Bailey-Lovie log MAR chart after refraction with autorefractor (Topcon KR-8000PA)

by an optometrist. The corneal assessment to ascertain keratoconus signs was carried out using Haag-Streit slit-lamp biomicroscope. The corneal mapping was conducted using a corneal topographer (Oculus Keratograph D-35582) and the central corneal thickness (CCT) was measured using anterior segment ocular coherence tomogram (Topcon 3D OCT-2000). A specialist established the keratoconus diagnosis based on the maximum corneal curvature (K_{\max}) of ≥ 50.00 Ds with topographic keratoconus classification (TKC) grading of >1.0 and the presence of classical keratoconus sign in either eye. The signs considered were Munson's sign, Rizutti's sign, Vogt striae, and Fleischer ring, in addition to scissors reflex on retinoscopy. The clinical details of the keratoconus and control group are presented in Table 1.

Table 1: Clinical attributes of keratoconus and control participants

Clinical parameters	Keratoconus ($n = 50$ eyes)	Control ($n = 50$ eyes)
Best-corrected visual acuity, log MAR, mean (SD), mean Snellen	0.21 (0.27), 6/9.6	-0.09 (0.06), 6/4.8
Refractive error (Sphere), diopter cylinder, mean (SD)	- 2.52 (2.85)	- 1.14 (1.61)
Refractive error (Cylindrical), diopter cylinder, mean (SD)	-3.45 (2.10)	-0.77 (0.90)
Maximum corneal curvature, dioptre, mean (SD)	54.48 (6.09)	45.66 (1.58)
Mean corneal curvature, dioptre, mean (SD)	47.03 (3.96)	44.51 (1.41)
Central corneal thickness, micrometre (μm), mean (SD)	495.34 (47.50)	554.36 (25.71)

Stimuli and procedure

The experimental stimulus was created and presented using MATLAB (32) software with psychtoolbox extensions (Psychtoolbox 3.0) (33, 34) and presented on a computer screen with the resolution of 1920 x 1080 pixels. The task combined vernier alignment and field matching techniques. The stimuli consisted of eight circles (suprathreshold acuity and contrast) each subtending 0.37° at the viewing distance of 90cm. The task for the observer was to align target circles with computer mouse click in relation to a reference line and circles presented against a 75% contrast grey background monocularly. At the start of the experiment a white central fixation circle (0.14°) and a white horizontal line were presented. This was followed by the presentation of a yellow reference circle

(0.37°) at the eccentricity of 0.73° from the central fixation (Figure 1; a). The task for the participant was to align a white target circle with the yellow reference circle at an equal distance from the horizontal reference line (Figure 1; a & b). After the placement of the first circle, the reference line was presented vertically, and the participant aligned the next target circle in the opposite field (Figure 1; b & c). Following this, the reference line was removed, and the participant placed another target circle to complete the remaining corner of a "virtual square" (Figure 1, d). Following this, two dots changed colour to orange (reference dots) and the task for the participant was to place the target circles at the mid-point and in alignment with these reference dots (Figure 1, e - g). The process continued until a square shape was completed by placing a total of seven target circles. (Figure 1, h). Participants fixated on a central target (0.14°) throughout the task. There was no time limit for the completion of the task. If the participant reported having made an error with the dot placement (e.g. mis-click), the researcher removed the dot to allow another attempt.

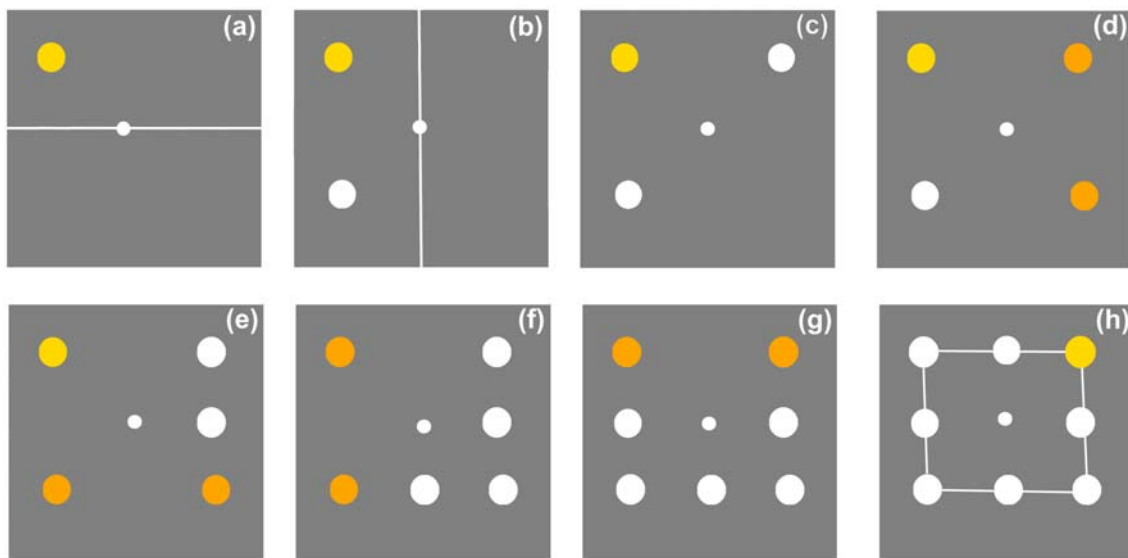


Figure 1: Schematic representation of the experimental task. The task was to position a supra-threshold contrast white circle in relation to the white line and/or yellow/orange circles to complete a square shape (bottom right panel).

a) Starting view for the participant (starting corner is randomised). Participant aligns a white dot (shown in b) with yellow dot on the opposite side of the white line to match the reference space.

b) Repeat of a) using vertical reference line and horizontal reference space.

c - d) Complete the square by aligning the remaining dots horizontally and vertically.

e) Fill in the space between the two orange dots in alignment with the central fixation target.

f - g) Repeat step e) on each side to finish reconstructing the square.

h) Final image shown to the participant after all clicks are completed.

Written informed consent was obtained from all participants once the nature of the experiment was explained. The experiment was completed monocularly with the patient's best correction in place in a dark room, with the computer monitor being the only light source. The distance from the monitor was controlled using head and chin rest. The task was repeated five times and the global distortion index (GDI) and global uncertainty index (GUI) were calculated as the mean and standard deviation respectively of local perceived misalignment of target circles over five trials. (30) The distortion data for both keratoconus and normal controls did not follow a normal distribution (Shapiro-Wilk test, $p < 0.001$) hence nonparametric statistics were used for all analyses. The study followed the tenets of Helsinki declaration on human research participants and the research protocol was approved by the Campus Research Ethics Committee of the Faculty of Health, St. Augustine campus, the University of the West Indies.

Results

The visual distortion measured as the global distortion index (GDI) was higher in keratoconus eyes ($n = 50$, median (M) = 0.43°) compared to the control eyes ($n = 50$, $M = 0.29^\circ$), Mann-Whitney $U = 756$, $z = -3.41$, $p = 0.001$. Similarly, the global uncertainty index (GUI) was also higher in keratoconus eyes ($n = 50$, $M = 0.39^\circ$) compared to the control eyes ($n = 50$, $M = 0.25^\circ$), Mann-Whitney $U = 763$, $z = -3.36$, $p = 0.001$. (Figure 2)

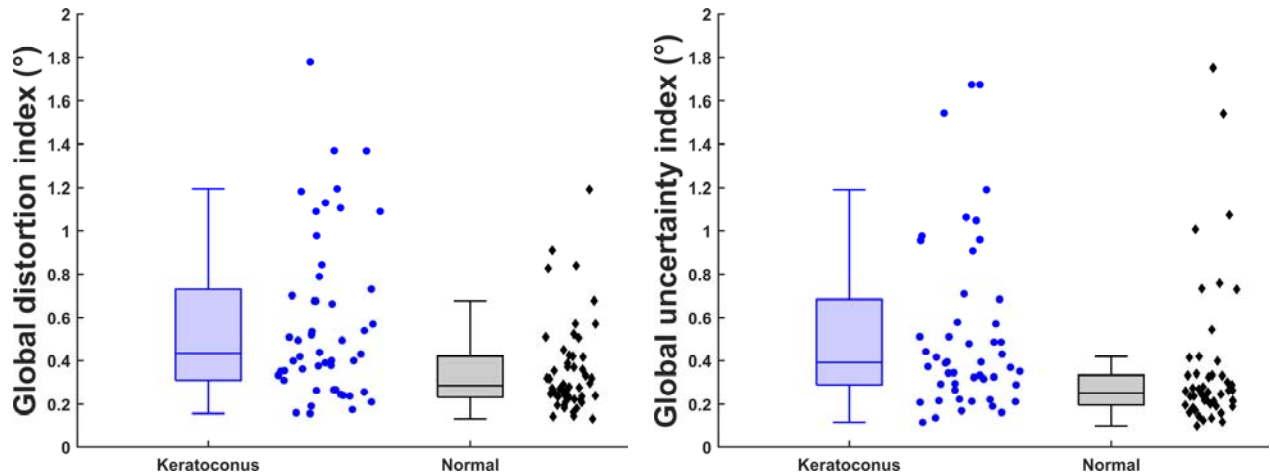


Figure 2: Boxplots comparing global distortion index (left panel) and global uncertainty index (right panel) between keratoconus eyes ($n = 50$) and normal eyes ($n = 50$). Box bounds: upper/lower quartile; horizontal bar within box bounds: median. All data points are also presented.

The relation between clinical parameters and distortion indices (GDI and GUI) were investigated using Spearman's rank order correlation. These are shown for GDI in Figure 3 and GUI in Figure 4 for BCVA (Figure 3a, 4a), maximum corneal curvature (Figure 3b, 4b), central corneal thickness (Figure 3c, 4c) and topographic keratoconus classification (TKC) scores (Figure 3d, 4d). Among the clinical parameters, BCVA strongly correlated with maximum corneal curvature (Spearman's ρ ($\rho = 0.73, p < 0.001$) and moderately correlated with TKC scores ($\rho = 0.49, p < 0.001$) but not with central corneal thickness ($\rho = -0.27, p = 0.06$). Thus, poorer BCVA was associated with greater maximum corneal curvature and TKC scores.

For the distortion indices, GDI was weakly correlated with BCVA ($\rho = 0.39, p = 0.005$, Figure 3a), moderately correlated with maximum corneal curvature ($\rho = 0.55, p < 0.001$, Figure 3b) and weakly correlated with TKC scores ($\rho = 0.32, p = 0.02$, Figure 3d). A moderate negative correlation was also observed between GDI and central corneal thickness ($\rho = -0.43, p = 0.002$, Figure 3c). Thus, higher GDI was associated with poorer BCVA, greater maximum corneal curvature and TKC scores, and lower central corneal thickness.

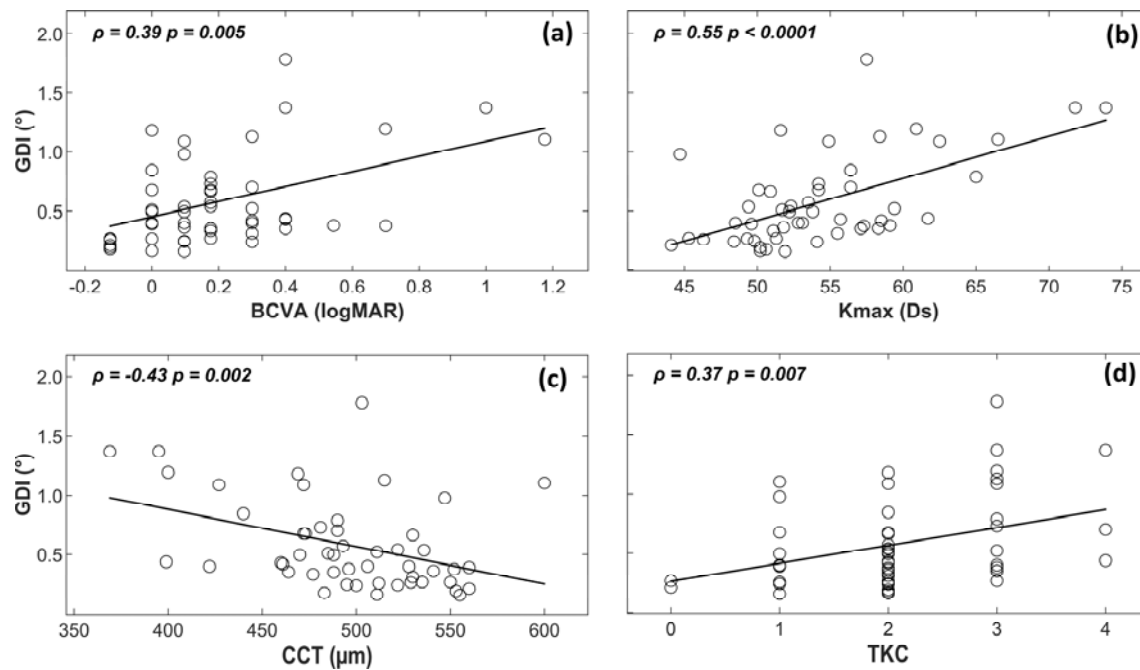


Figure 3: The scatterplots showing correlation between global distortion index (GDI) with a) the best corrected visual acuity (BCVA), b) maximum corneal curvature (K_{max}), c) central corneal thickness (CCT), and d) topographic keratoconus classification (TKC). The red line represents least square regression line. The Spearman's rho (ρ) and the p value are also provided.

The global uncertainty index (GUI) also exhibited a weak positive correlation with BCVA ($\rho = 0.35, p = 0.01$, Figure 4a), moderate correlation with maximum corneal curvature ($\rho = 0.53, p < 0.001$, Figure 4b) and weak correlation with TKC scores ($\rho = 0.32, p = 0.02$, Figure 4d). A moderate negative correlation was also observed between the GUI and the central corneal thickness (CCT) ($\rho = -0.44, p = 0.001$, Figure 4c). Thus, higher GUI was associated with poorer BCVA, greater maximum corneal curvature and TKC scores, and lower central corneal thickness.

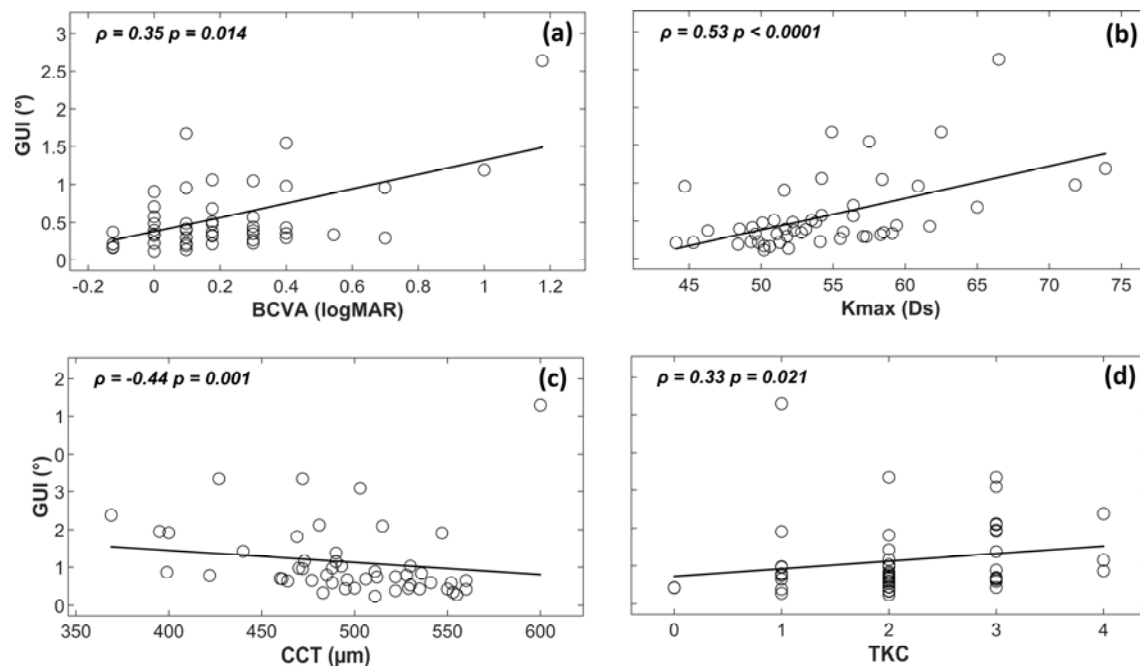


Figure 4: The scatterplots showing correlation between global uncertainty index (GUI) with a) the best-corrected visual acuity (BCVA), b) maximum corneal curvature (K_{\max}), c) central corneal thickness (CCT), and d) topographic keratoconus classification (TKC). The red line represents least square regression line. The Spearman's rho (ρ) and the p value are also provided.

Discussion

This study for the first time quantitatively evaluated visual distortion experienced in keratoconus. The results showed that visual distortion was higher in individuals with keratoconus compared to the normally sighted controls. The distortion indices also correlated with commonly measured clinical metrics of keratoconus such as K_{\max} and TKC.

The results demonstrate that measurements of visual distortion obtained with our paradigm differentiate individuals with keratoconus from those without. A similar paradigm based on vernier alignment has been used to measure perceptual distortion in amblyopia and AMD before. (30, 31, 35, 36) However these tests are lengthy to conduct in a clinical setting compared to the combined vernier alignment and field matching task used in the current study, which takes just a few minutes to

complete. This renders our paradigm a more viable option for characterising visual distortions associated with keratoconus in clinical settings.

Both GDI and GUI increased with worsening visual acuity, albeit the correlation was weak. Using similar methods of distortion quantification, distortions were found to be higher in the amblyopic population compared to non-amblyopic controls. (30, 35) Amblyopic observers experience chronic distortion during development and may learn the spatial form of distorted optotypes. In contrast, AMD patients have an acquired deficit later in life and visual distortion (metamorphopsia) arises at the retinal level. Although research concerning the underlying basis of metamorphopsia in these patient groups continues to be limited, it has been suggested that the visual processing stream in such instances may be subject to top-down influences as a result of the slow progressing nature of the aetiologies, potentially resulting in some degree of visual adaptation to the degraded image quality and a resulting dissociation of perceived metamorphopsia from the visual acuity deficit. (31) Such influences may also explain why we found a higher GUI (index of stability of the visual percept) that correlated with certain clinical keratoconus indices.

In our sample, poorer BCVA was associated with greater maximum corneal curvature ($\rho = 0.73$) and TKC scores ($\rho = 0.49$) but was not significantly correlated with CCT ($\rho = -0.27$). Previous studies have shown that visual acuity shows a variable degree of correlation with the corneal structural measures and vision related quality of life in keratoconus. (9-11, 37) In comparison, contrast sensitivity has been found to correlate with corneal irregularities (37), higher order aberrations (13), and vision related quality of life (12). However, proper measurement of contrast sensitivity is time consuming and traditional clinical tests of contrast sensitivity such as VisTech chart have limited spatial frequencies for evaluation of moderate to advanced keratoconus. (15) Hence, the distortion test used in the current study could provide an alternative or adjunctive visual measure for keratoconus.

The visual distortion indices also correlated with commonly measured corneal structural parameters. Both GDI and GUI increased with higher corneal curvature, higher TKC and lower corneal thickness. The maximum corneal curvature (K_{\max}) and central corneal thickness better reflect the quality of life measures in keratoconus compared to visual acuity. (38, 39) Distortion measurement could therefore serve as a helpful bridge between clinical indicators and perceived quality of life that is quick and simple to administer.

In recent times home monitoring of different ocular conditions have been used (31, 40, 41) and these have become even more important due to the COVID-19 pandemic, during which it has been necessary in many instances to constrain in-person clinical interactions to essential care. Various home-based applications implemented on the digital devices show good reliability compared to the hospital-based tests for different ocular conditions. (40-44) As far as we are aware, there are no systematic measures of distortion in keratoconus that could be utilised in this context. Proper monitoring in keratoconus could ensure timely medical intervention such as collagen crosslinking but requires assessment by an eye care professional using specialist imaging equipment. A simple monocular visual task such as that used in the current study could be easily transformed into a home-based tool. This also holds promise for individuals living with keratoconus in remote or rural areas with limited specialist access. In future, we will develop a version of the distortion test for use on personal or portable computing devices, to explore the use of the test as a home based tool for keratoconus.

Some limitations can be identified for our study. Firstly, our paradigm provides information about distortion magnitude, but less about the individual's subjective percept, e.g. magnification, barrel distortion, etc. If clinically relevant, practitioners can store the square drawings to retain as a way of visually monitoring distortion over time. However, at present we are not able to offer a systematic method for detecting significant changes in the shape of the constructed square, which has the capacity to change significantly while yielding similar GDI and GUI measurements. This could be developed in future using image processing techniques or through methods such as subdivision into

quadrant-based GDI and GUI measurements. Additionally, the value of a measurement tool to detect progression of keratoconus remediation following treatment will depend on the repeatability of distortion measurements, which is the focus of future work. Secondly, this was a cross-sectional study and we are unable to provide information about the extent to which treatments for keratoconus such as cross-linking may affect such measurements. As the correlation between BCVA and our distortion measures was modest, we cannot be certain whether interventions to improve visual acuity will impact GDI and GUI. As such, whether these distortion measures could be used to support clinical decision-making about keratoconus interventions or as a treatment outcome measure should be a focus of future work.

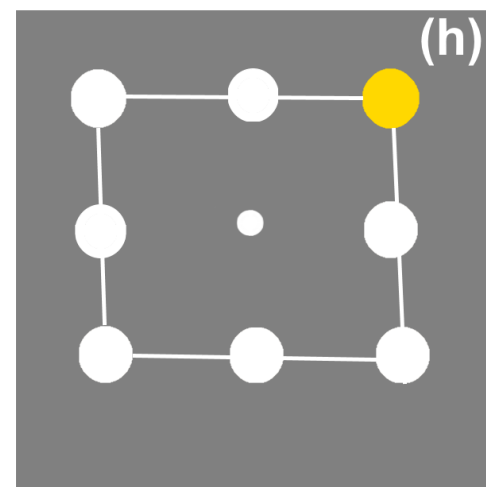
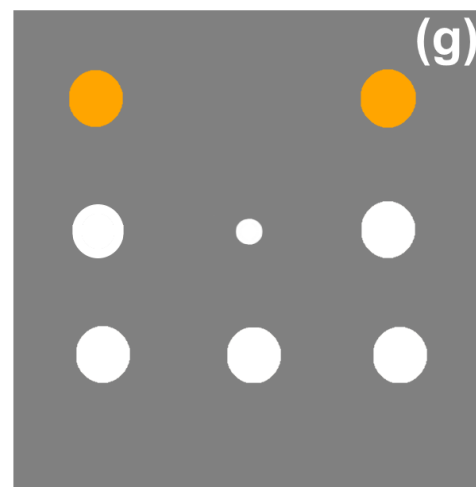
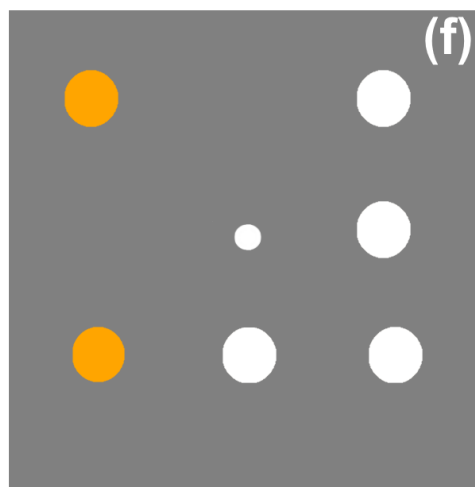
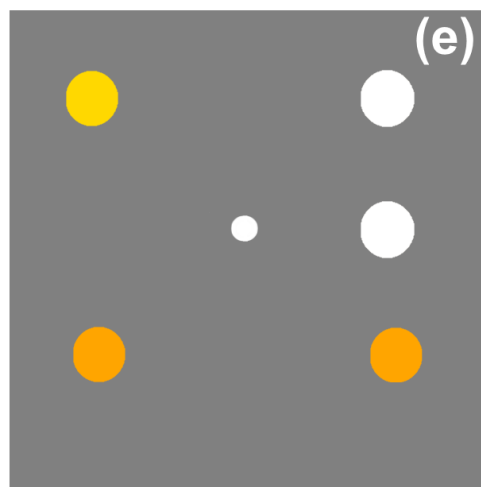
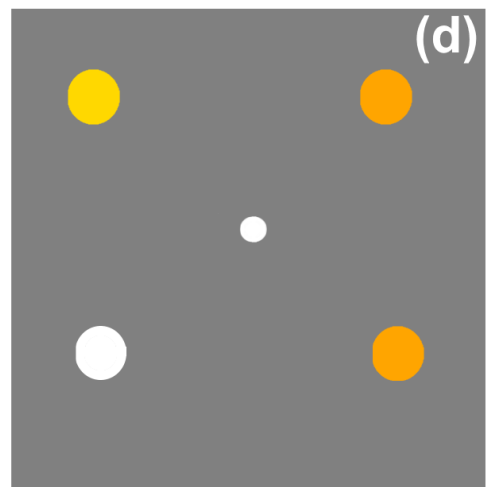
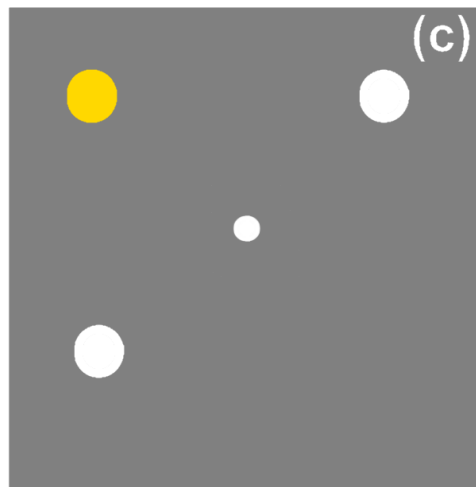
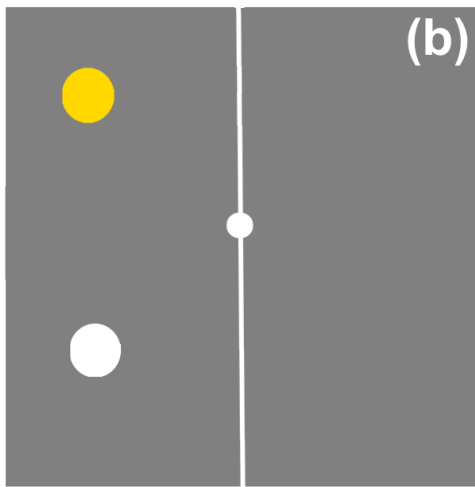
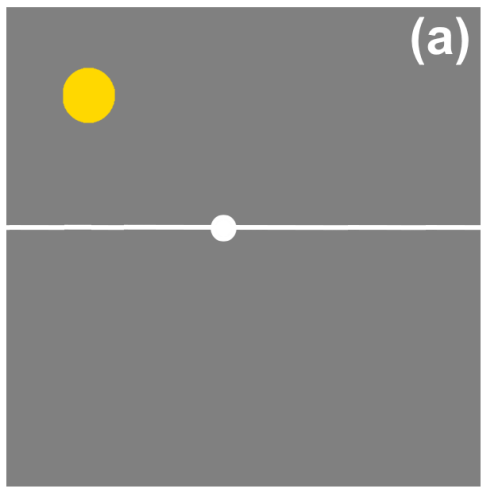
References

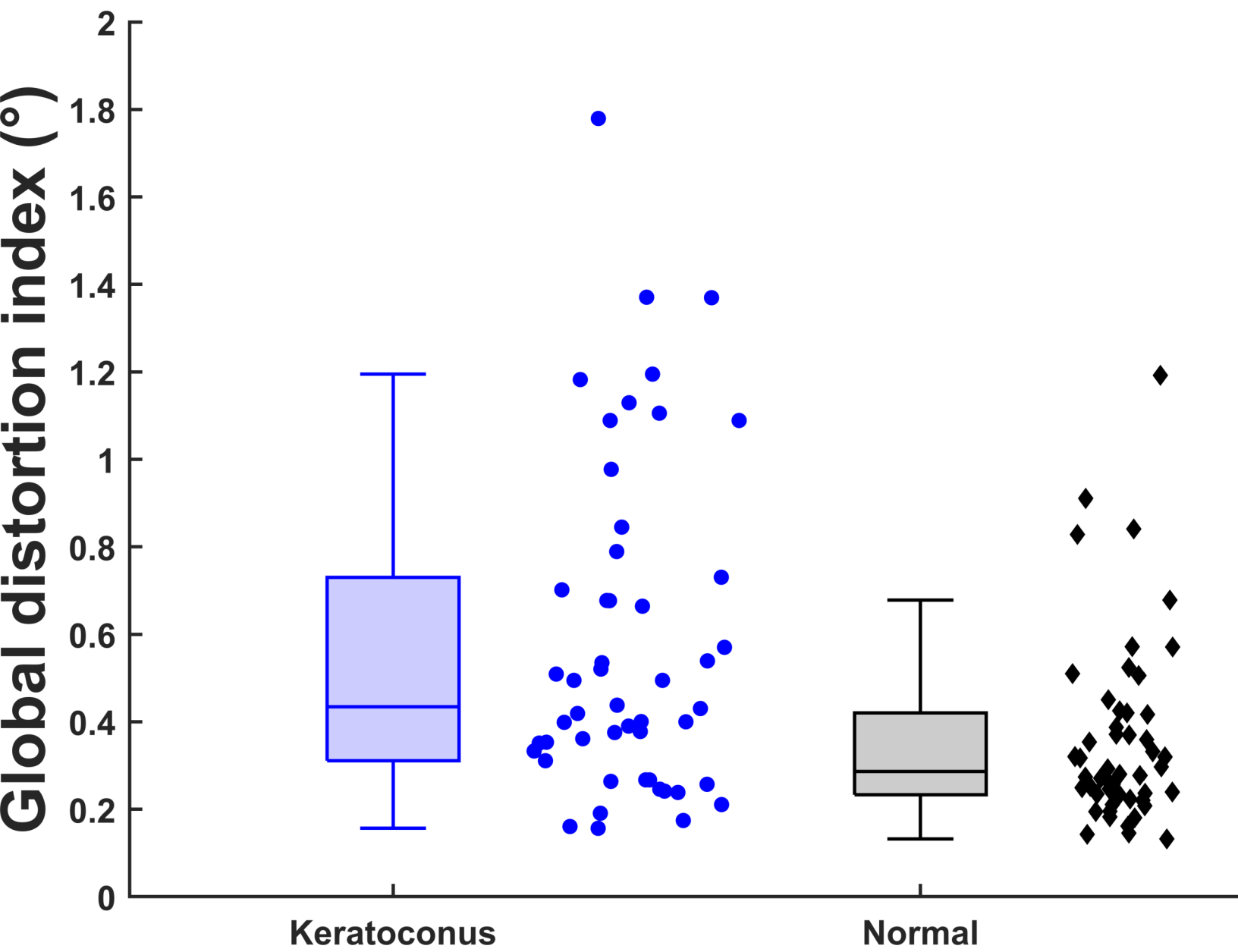
1. Loh IP, Sherwin T. Is Keratoconus an Inflammatory Disease? The Implication of Inflammatory Pathways. *Ocular Immunology and Inflammation*. 2022;30(1):246-55.
2. Wisse RP, Kuiper JJ, Gans R, Imhof S, Radstake TR, Van der Lelij A. Cytokine Expression in Keratoconus and its Corneal Microenvironment: A Systematic Review. *Ocul Surf*. 2015;13(4):272-83.
3. Chan E, Chong EW, Lingham G, Stevenson LJ, Sanfilippo PG, Hewitt AW, et al. Prevalence of Keratoconus Based on Scheimpflug Imaging: The Raine Study. *Ophthalmology*. 2021;128(4):515-21.
4. Godefrooij DA, de Wit GA, Uiterwaal CS, Imhof SM, Wisse RP. Age-specific Incidence and Prevalence of Keratoconus: A Nationwide Registration Study. *Am J Ophthalmol*. 2017;175:169-72.
5. Edwards M, McGhee CNJ, Dean S. The genetics of keratoconus. *Clinical & Experimental Ophthalmology*. 2001;29(6):345-51.
6. Applegate RA, Hilmantel G, Howland HC, Tu EY, Starck T, Zayac EJ. Corneal first surface optical aberrations and visual performance. *Journal of refractive surgery (Thorofare, NJ : 1995)*. 2000;16(5):507-14.
7. Okamoto C, Okamoto F, Samejima T, Miyata K, Oshika T. Higher-order wavefront aberration and letter-contrast sensitivity in keratoconus. *Eye*. 2008;22(12):1488-92.
8. Rabinowitz YS. Keratoconus. *Survey of Ophthalmology*. 1998;42(4):297-319.
9. Steinberg J, Bußmann N, Frings A, Katz T, Druchkiv V, Linke SJ. Quality of life in stable and progressive 'early-stage' keratoconus patients. *Acta Ophthalmologica*. 2020;n/a(n/a).
10. Kymes SM, Walline JJ, Zadnik K, Gordon MO. Quality of life in keratoconus. *American Journal of Ophthalmology*. 2004;138(4):527-35.
11. Sahebzada S, Fenwick EK, Xie J, Snibson GR, Daniell MD, Baird PN. Impact of Keratoconus in the Better Eye and the Worse Eye on Vision-Related Quality of Life. *Invest Ophthalmol Vis Sci*. 2014;55(1):412-6.
12. Kandel H, Pesudovs K, Watson SL. Measurement of Quality of Life in Keratoconus. *Cornea*. 2020;39(3).
13. Shneor E, Piñero DP, Doron R. Contrast sensitivity and higher-order aberrations in Keratoconus subjects. *Scientific Reports*. 2021;11(1):12971.

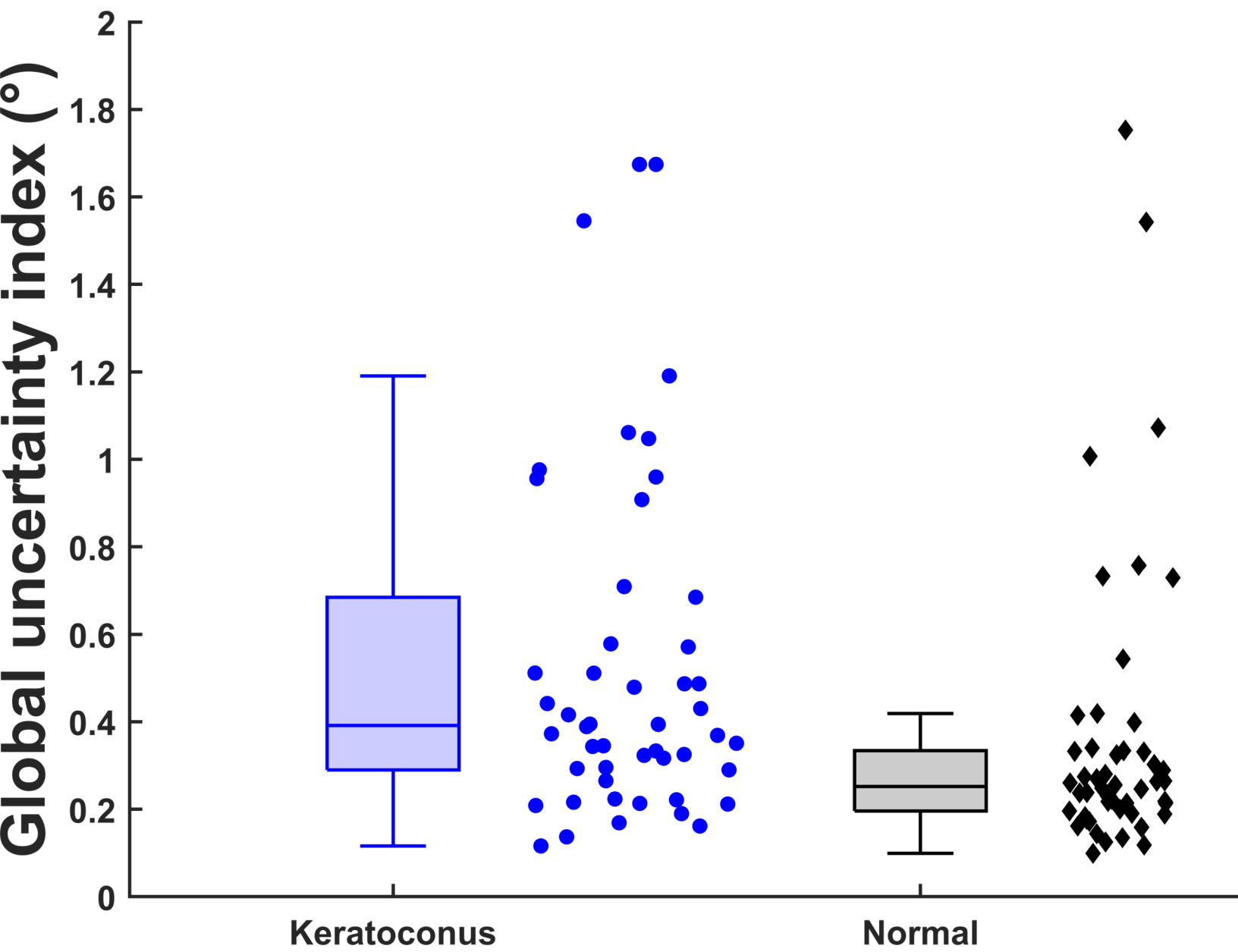
14. Maeda N, Sato S, Watanabe H, Inoue Y, Fujikado T, Shimomura Y, et al. Prediction of letter contrast sensitivity using videokeratographic indices. *American Journal of Ophthalmology*. 2000;129(6):759-63.
15. Zadnik K, Mannis MJ, Johnson CA, Rich D. Rapid contrast sensitivity assessment in keratoconus. *Am J Optom Physiol Opt*. 1987;64(9):693-7.
16. Raiskup-Wolf F, Hoyer A, Spoerl E, Pillunat LE. Collagen crosslinking with riboflavin and ultraviolet-A light in keratoconus: Long-term results. *Journal of Cataract & Refractive Surgery*. 2008;34(5):796-801.
17. Vinciguerra P, Albè E, Trazza S, Rosetta P, Vinciguerra R, Seiler T, et al. Refractive, Topographic, Tomographic, and Aberrometric Analysis of Keratoconic Eyes Undergoing Corneal Cross-Linking. *Ophthalmology*. 2009;116(3):369-78.
18. Pérez-Rueda A, Castro-Luna G. A model of visual limitation in patients with keratoconus. *Scientific Reports*. 2020;10(1):19335.
19. Esaka Y, Kojima T, Dogru M, Hasegawa A, Tamaoki A, Uno Y, et al. Prediction of Best-Corrected Visual Acuity With Swept-Source Optical Coherence Tomography Parameters in Keratoconus. *Cornea*. 2019;38(9):1154-60.
20. Wisse RPL, Simons RWP, van der Vossen MJB, Muijzer MB, Soeters N, Nuijts RMMA, et al. Clinical Evaluation and Validation of the Dutch Crosslinking for Keratoconus Score. *JAMA Ophthalmology*. 2019;137(6):610-6.
21. Goldstein M, Loewenstein A, Barak A, Pollack A, Bukelman A, Katz H, et al. Results of a multicenter clinical trial to evaluate the preferential hyperacuity perimeter for detection of age-related macular degeneration. *Retina*. 2005;25(3):296-303.
22. Pitrelli Vazquez N, Knox PC. Assessment of visual distortions in age-related macular degeneration: emergence of new approaches. *Br J Ophthalmol*. 2015;12:9-15.
23. Pitrelli Vazquez N, Harding SP, Heimann H, Czanner G, Knox PC. Radial shape discrimination testing for new-onset neovascular age-related macular degeneration in at-risk eyes. *PLoS One*. 2018;13(11):e0207342-e.
24. Wang Y-Z, Wilson E, Locke KG, Edwards AO. Shape Discrimination in Age-Related Macular Degeneration. *Invest Ophthalmol Vis Sci*. 2002;43(6):2055-62.
25. Westheimer G. Visual acuity and hyperacuity: resolution, localization, form. *Am J Optom Physiol Opt*. 1987;64(8):567-74.
26. Westheimer G. The spatial sense of the eye. Proctor lecture. *Invest Ophthalmol Vis Sci*. 1979;18(9):893-912.
27. Fang MS, Enoch JM, Lakshminarayanan V, Kim E, Kono M, Strada E, et al. The three point vernier alignment or acuity test (3Pt VA test): an analysis of variance. *Ophthalmic & physiological optics : the journal of the British College of Ophthalmic Opticians (Optometrists)*. 2000;20(3):220-34.
28. McKendrick AM, Johnson CA, Anderson AJ, Fortune B. Elevated Vernier Acuity Thresholds in Glaucoma. *Invest Ophthalmol Vis Sci*. 2002;43(5):1393-9.
29. Little J-A, Woodhouse JM, Lauritzen JS, Saunders KJ. Vernier Acuity in Down Syndrome. *Invest Ophthalmol Vis Sci*. 2009;50(2):567-72.
30. Piano MEF, Bex PJ, Simmers AJ. Perceptual Visual Distortions in Adult Amblyopia and Their Relationship to Clinical Features. *Invest Ophthalmol Vis Sci*. 2015;56(9):5533-42.
31. Wiecek E, Lashkari K, Dakin SC, Bex P. Novel Quantitative Assessment of Metamorphopsia in Maculopathy. *Invest Ophthalmol Vis Sci*. 2015;56(1):494-504.
32. MATLAB. 8.1.0.604 (R2013a). Natick, Massachusetts: The MathWorks Inc.; 2013.
33. Brainard DH. The Psychophysics Toolbox. *Spatial Vision*. 1997;10(4):433-6.
34. Kleiner M, Brainard D, Pelli D, Ingling A, Murray R, Broussard C. What's new in Psychtoolbox-3? *Perception*. 2007;36:1-16.
35. Piano MEF, Bex PJ, Simmers AJ. Perceived Visual Distortions in Juvenile Amblyopes During/Following Routine Amblyopia Treatment. *Invest Ophthalmol Vis Sci*. 2016;57(10):4045-54.

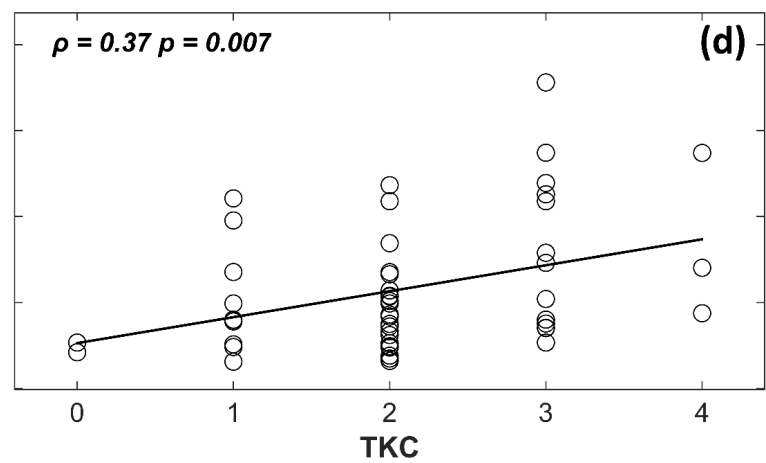
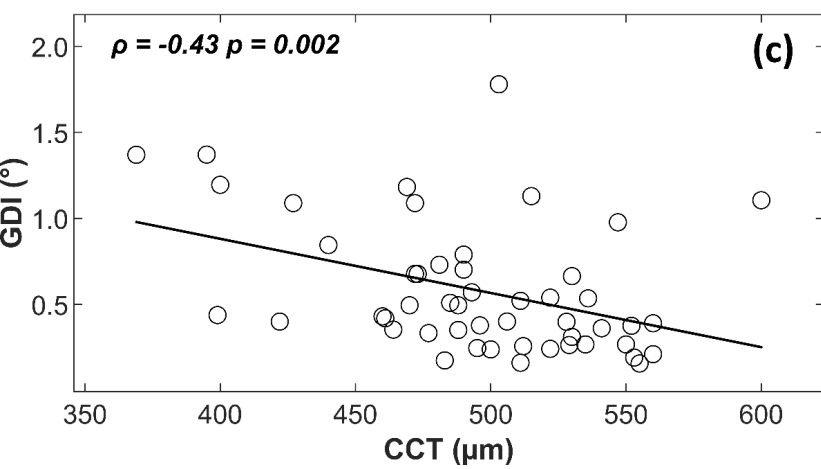
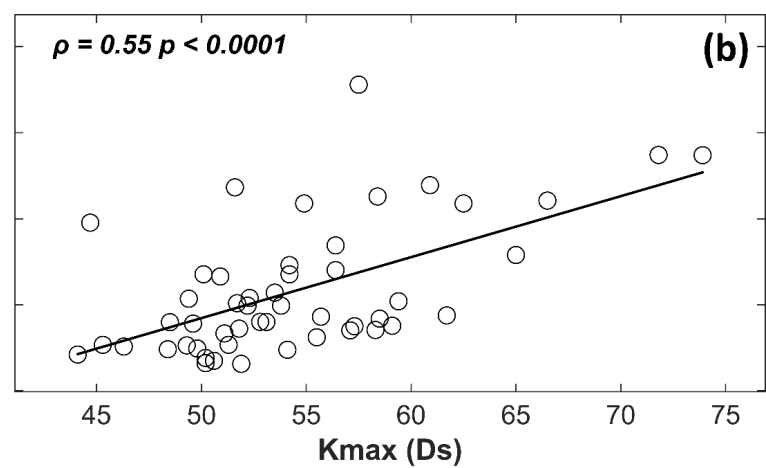
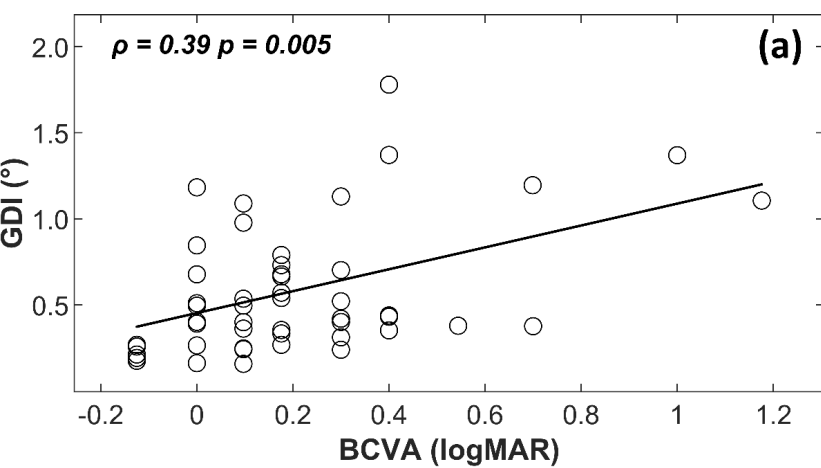
36. Loewenstein A, Malach R, Goldstein M, Leibovitch I, Barak A, Baruch E, et al. Replacing the Amsler grid: A new method for monitoring patients with age-related macular degeneration¹¹ Drs. Loewenstein, Malach, Alster, and Rafael: acknowledge a financial interest in Notal Vision. *Ophthalmology*. 2003;110(5):966-70.
37. Liduma S, Luguzis A, Krumina G. The impact of irregular corneal shape parameters on visual acuity and contrast sensitivity. *BMC Ophthalmology*. 2020;20(1):466.
38. Kymes SM, Walline JJ, Zadnik K, Sterling J, Gordon MO. Changes in the Quality-of-Life of People with Keratoconus. *American Journal of Ophthalmology*. 2008;145(4):611-7.e1.
39. Saunier V, Mercier A-E, Gaboriau T, Malet F, Colin J, Fournié P, et al. Vision-related quality of life and dependency in French keratoconus patients: Impact study. *Journal of Cataract & Refractive Surgery*. 2017;43(12):1582-90.
40. Ward E, Wickens RA, O'Connell A, Culliford LA, Rogers CA, Gidman EA, et al. Monitoring for neovascular age-related macular degeneration (AMD) reactivation at home: the MONARCH study. *Eye*. 2021;35(2):592-600.
41. Che Hamzah J, Daka Q, Azuara-Blanco A. Home monitoring for glaucoma. *Eye*. 2020;34(1):155-60.
42. Aboobakar IF, Friedman DS. Home Monitoring for Glaucoma: Current Applications and Future Directions. *Seminars in Ophthalmology*. 2021;36(4):310-4.
43. Jones PR, Campbell P, Callaghan T, Jones L, Asfaw DS, Edgar DF, et al. Glaucoma Home Monitoring Using a Tablet-Based Visual Field Test (Eyecatcher): An Assessment of Accuracy and Adherence Over 6 Months. *American Journal of Ophthalmology*. 2021;223:42-52.
44. Chaikitmongkol V. Home Monitoring for Age-Related Macular Degeneration. In: Chhablani J, editor. *Choroidal Neovascularization*. Singapore: Springer Singapore; 2020. p. 363-73.

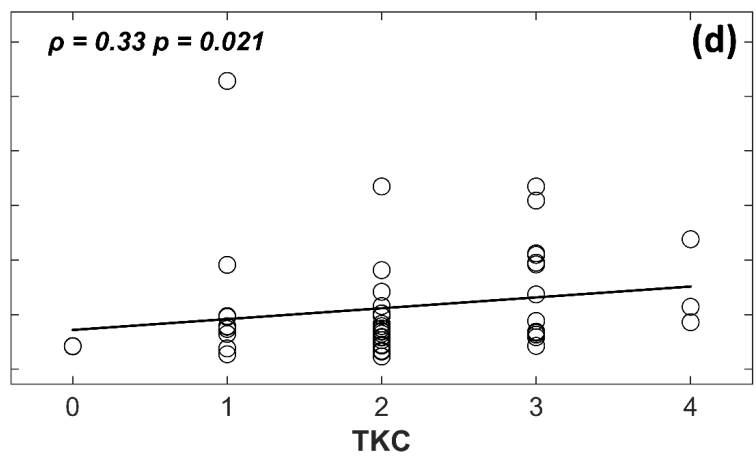
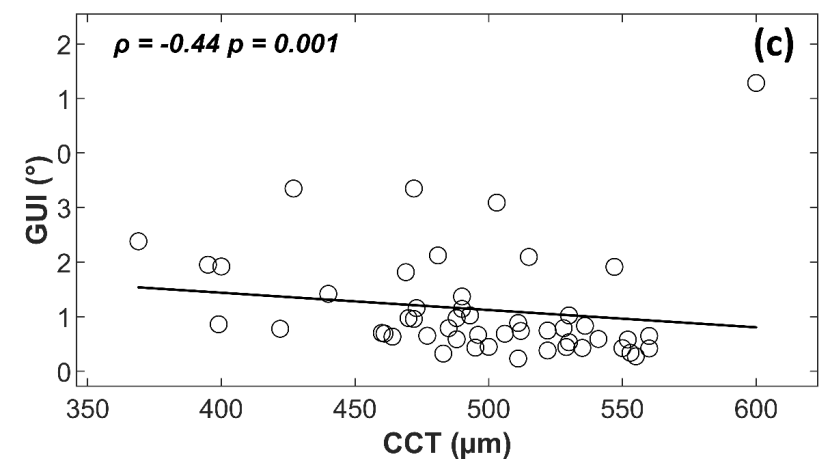
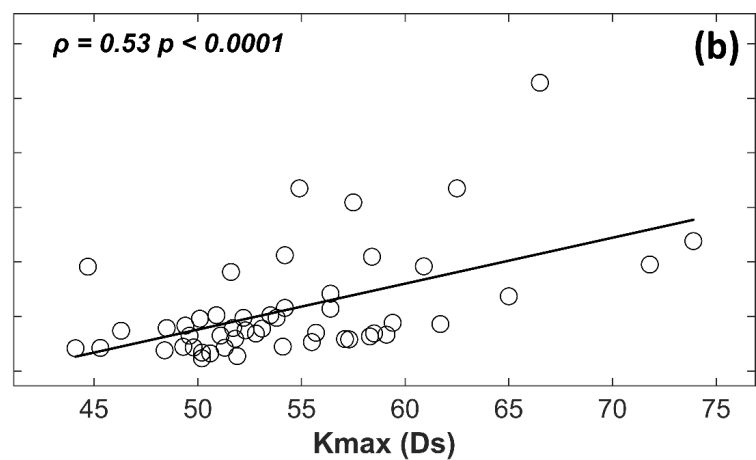
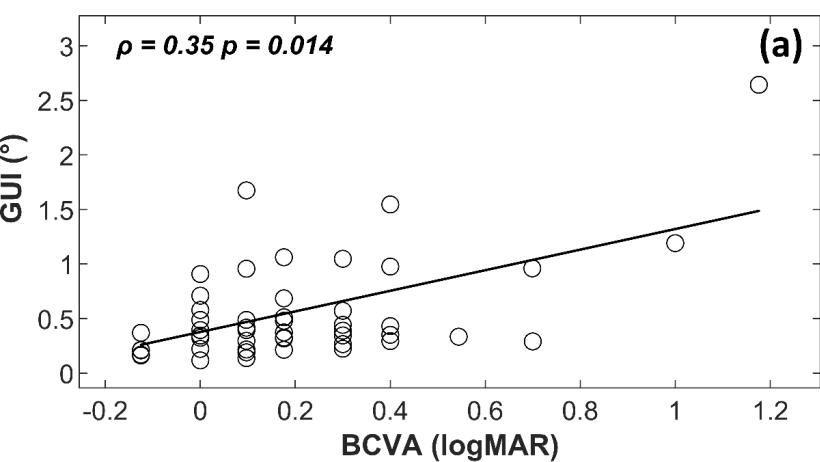
366











Clinical parameters	Keratoconus (<i>n</i> = 50 eyes)
Best-corrected visual acuity, log MAR, mean (SD)	0.21 (0.27)
Refractive error (Sphere), diopter cylinder, mean (SD)	- 2.52 (2.85)
Refractive error (Cylindrical), diopter cylinder, mean (SD)	-3.45 (2.10)
Maximum corneal curvature, dioptre, mean (SD)	54.48 (6.09)
Mean corneal curvature, dioptre, mean (SD)	47.03 (3.96)
Central corneal thickness, micrometre (μm), mean (SD)	495.34 (47.50)

Control ($n = 50$ eyes)

-0.09 (0.06)

- 1.14 (1.61)

-0.77 (0.90)

45.66 (1.58)

44.51 (1.41)

554.36 (25.71)
